

# HYDROTHERMAL SYNTHESIS AND CHARACTERIZATION OF BOEHMITE/TITANIA HYBRID MATERIALS ON COTTON FABRICS

MING-SHIEN YEN\*, MU-CHENG KUO, CHENG-WEI YEH and YEN-SHENG CHENG

*Department of Materials Engineering, Kun Shan University, Tainan 71003,  
Taiwan, Republic of China*

*Received May 10, 2012*

A series of novel boehmite/titania hybrid materials was synthesized from aluminum isopropoxide and titanium-n-butoxide using a hydrothermal synthesis process. Grey cotton fabrics were dyed, and the hybrid materials were combined with the pre-treated cotton fabrics through a padding-drying-curing process. The structures of the hybrid materials were analyzed using FTIR and  $^{27}\text{Al}$ -NMR. Moreover, the morphological structures of the processed cotton fabrics were evaluated using scanning electron microscopy (SEM) and energy dispersive spectrometer (EDS) analyses. Our data show that the electric conductivity of the processed cotton fabrics was improved in the fabrics processed with a higher amount of aluminum isopropoxide and all the processed fabrics had a good water repellent performance.

**Keywords:** boehmite, titania, hydrothermal, cotton fabrics, conductivity, water repellent

## INTRODUCTION

Inorganic-organic composite materials with well-defined nanostructures have gained interest due to their improved properties resulting from the combination of two components in one uniform material.<sup>1,2</sup> In recent years, the hydrothermal technology has been used to fabricate functional composite materials, such as mesoporous materials, photocatalysts, nanoparticles, inorganic powders, and gas sensors.<sup>3-8</sup> Materials composed of both organic and inorganic components possess the flexibility characteristic of organic materials and the wear resistance, aging resistance, and resistance to elements specific to inorganic materials. The surface quality of organic materials can be improved with this type of composite materials. Further, the range of applications can be expanded.<sup>9-12</sup> Organic-inorganic hybrid materials are also adopted to prepare multifunctional polymeric materials.<sup>13-15</sup>

With the development and advancement of photochemical technology, more attention has been paid to improving UV resistance, air purification, water disinfection, and the anti-bacterial properties of materials using semiconductor oxides for

photocatalytic technology and chemical stability.<sup>16-20</sup> Titanium dioxides (rutile; R type, anatase; A type and brookite) are inexpensive and non-toxic without potential for secondary pollution, and they are characterized by high catalytic activity, high oxidation capacity, and stable biological, chemical, and photochemical properties. The hydroxyl free radicals produced from the photocatalytic processing of titanium dioxides can help in killing bacteria and viruses and in damaging other organic matter. The mechanism of the photocatalytic activity of  $\text{TiO}_2$  has been studied previously.<sup>21,22</sup> The most widely accepted mechanism is the migration of a valence electron to the conduction band and the formation of electron-hole pairs, which react with the adsorbed molecules at the semiconductor surface, resulting in the degradation of the adsorbates.<sup>23</sup>

An inorganic sol is blended with an organic polymer solution and then gelatinized. The organic monomer and the inorganic sol are polymerized simultaneously using a hybridization method to form an interpenetrating network. The major structural feature of this composite material is that

the microzones are of the order of nanometers and can be interpenetrating.<sup>24,25</sup> The  $\gamma$ -AlOOH coating is a thin layer material that adheres to a parent material to play a special role, and it provides a certain anchoring strength to the parent material. It can overcome some types of defects in the parent material and improve the material's surface characteristics, such as optical and electrical characteristics, erosion and corrosion resistance, wearability, and mechanical strength. It is a film with support. There are many preparation methods for the coating material and they can be classified into two major types: physical processes, such as the vapor deposition method and the sputtering method, and chemical processes, such as chemical vapor deposition, spray pyrolysis, sol-gel, and hydrothermal methods.<sup>26-28</sup> At present, it is known that  $\gamma$ -AlOOH can induce improved hardness, thermal stability, corrosion resistance, high surface activity, anti-oxidation properties, high ductility, and high tenacity, and although it is mostly applied to ceramics as a substrate, it has been recently applied to other materials too.<sup>29-31</sup>

Therefore, this study adopted the hydrothermal method to synthesize a series of composite materials of tetrabutyl titanate and aluminum isopropoxide. These composite materials were used for the post-finished processing of cotton fabrics to form network structures. Finally, for the processed fabrics with various ratios of composite materials, electric conductivity and water repellency tests were conducted to assess all types of properties in order to evaluate the benefits of multi-functionality.

## EXPERIMENTAL

### Materials

Desized, scoured, and bleached plain-weave cotton fabrics [ends (100)\*picks (56)/(32<sup>s</sup>/1)\*(32<sup>s</sup>/1)] were supplied by Everest Textile Industry Co., Ltd., Tainan. Tetrabutyl titanate (TBT) and aluminum isopropoxide (AIP) were purchased from Acros Co., Ltd., Junghe, Belgium. Sodium sulfate and sodium carbonate were purchased from Hayashi Pure Chemical Co., Ltd., Osaka, Japan. The reactive dye (Everzol Navy Blue EBN) was supplied by Everlight Chemical Industrial Co., Ltd., Taipei, Taiwan. The scouring agent laundry detergent (Lipofol TM-1000E) was supplied by Taiwan Nicca Chemical Industrial Co., Ltd., Taipei, Taiwan.

### Preparation and process

#### *Dyeing of cotton fabrics*

Cotton fabrics were dyed using an infra-red dyeing machine (LOGIC ART, LA-650) at a liquor ratio of 1:40

with distilled water. The dyeing bath was prepared with a reactive dye concentration of 2% o.w.f., 20 g L<sup>-1</sup> of sodium sulfate, and 10 g/L of sodium carbonate. Dyeing began at 30 °C for 10 min, and then the dye bath temperature was increased at a rate of 2 °C/min to 60 °C and maintained at this temperature for 40 min; the temperature was then decreased to 40 °C. After dyeing, the fabrics were placed in a 2 g L<sup>-1</sup> scouring agent liquor at 80 °C for 20 min for two washings and then dried at room temperature.

#### *Preparation of hybrid materials*

For boehmite synthesis, the boehmite sol solution derived from aluminum isopropoxide (Al(OCH<sub>3</sub>)<sub>3</sub>) was prepared according to the method reported by Yoldas.<sup>32</sup> Al(OCH<sub>3</sub>)<sub>3</sub> was hydrolyzed in excess deionized water (nH<sub>2</sub>O:nAl(OCH<sub>3</sub>)<sub>3</sub> = 100:1) for 1 h under vigorous stirring at 80 °C. Peptization was initiated by adding HNO<sub>3</sub>; (nAl(OCH<sub>3</sub>)<sub>3</sub>:nHNO<sub>3</sub> = 1:0.1). Subsequently, the resulting colloidal suspension was heated under reflux for 2 h with vigorous stirring at 80 °C. A viscous boehmite sol solution was produced. The various proportions of tetrabutyl titanate (TBT) were prepared by adding 50 mL of deionized water to 50 mL of ethanol (99%) and then using 2N HCl to adjust the pH to 3.5 with vigorous stirring. Finally, the boehmite sol solution and premixed TBT solution were fabricated and stirred by a hydrothermalclave system at 100 °C for 6 h to generate hybrid materials A<sub>1</sub>–A<sub>4</sub> with molar ratios of 1:0.5, 1:1, 1:1.5, 1:2. Alternatively, the boehmite sol and premixed TBT solutions were mixed and stirred according to the procedure applied for hybrid materials A<sub>1</sub>–A<sub>4</sub> to generate hybrid materials T<sub>1</sub>–T<sub>4</sub> with molar ratios of 0.5:1, 1:1, 1.5:1, and 2:1. The co-hydrolysis of different molar concentrations of aluminum isopropoxide (AIP) and TBT occurred during mixing.

#### *Processing of hybrid materials*

The treatment of 25 cm × 20 cm pieces of the cotton fabrics was performed using the “two dips, two nips” padding method with a pick-up of 80%. The typical padding solution was prepared as follows: fabrics were dipped for 3 min in a process solution containing the required weight percent of hybrid materials. A padding-drying-curing procedure was used to disaggregate the agglomerated particles into well-dispersed colloidal particles. Fumed boehmite and titania sol-treated fabric samples were padded and nipped to remove excess liquid and to obtain a percent wet pick-up of 80% using a padder (Rapid Labortex Co., Ltd., Taoyuan, Taiwan) with a set nipping pressure. The treated fabric was pre-dried in an oven at 80 °C for 5 min. Then, the processed fabrics were cured at 150 °C for 120 s in a preheated curing oven (Chang Yang R3). The fabrics were rinsed with water several times to thoroughly remove any hybrid material residue and dried

at 80 °C for 5 min before they were evaluated. Processed fabrics CA<sub>1</sub>–CA<sub>4</sub> and CT<sub>1</sub>–CT<sub>4</sub> denote grey cotton fabrics dyed with hybrid materials A<sub>1</sub>–A<sub>4</sub> and T<sub>1</sub>–T<sub>4</sub>, respectively.

### Methods and characterization

FT-IR spectra were recorded on a Bio-Rad Digilab FTS-40 spectrometer (KBr). The <sup>27</sup>Al-NMR spectra were collected using a Bruker Advance 500 MHz NMR spectrometer at 78.49 MHz with a recycle time of 60 s; the number of scans was 914. The surface morphology of the processed cotton fabrics was investigated using a field-emission scanning electron microscope (FE-SEM, Philips XL40). The elemental analysis was carried out using a Philips XL40 FEG-Energy Dispersive X-ray Spectrometer. The weathering properties of the processed textiles were evaluated in accordance with ASTM G154 Cycle 1 testing methods, using a Q-Panel Lab Products QUV-LU-8047. The electric conductivity of the processed cotton fabrics, whose width of species is 1000 mm, was analyzed using a high-impedance meter (Mitsubishi, MCP HT450). The operating voltage was 10 V, and the selecting probe used URS with a test time of 1 min. The color strength and evenness of the processed textiles were measured using a Hunter Lab Corporation spectrophotometer (Mini Scan XE Plus/Color Flex, 4000S, D/8). Water contact angle measurements were made with a water contact angle meter (Sigma CAM100). The washing fastness was evaluated by the AATCC Test Method 61-2001 Test No. 2A, using an AATCC Standard Instrumental Logic Art LA-650 Infrared Dyer.

### Determination of color strength and related parameters

The reflectance values of the treated samples were measured using an ultraviolet-visible (UV-Vis) spectrophotometer (UV-1201, Shimadzu) at λ<sub>max</sub>. K/S values were determined using the Kubelka-Munk equation:<sup>33</sup>

$$\frac{K}{S} = \frac{(1 - R_{\lambda_{\max}})^2}{2R_{\lambda_{\max}}}$$

where K is the coefficient of absorption, S is the coefficient of scattering, and R<sub>λ<sub>max</sub></sub> is the reflectance value of the fabric at peak wavelength.

The color differences and relative color strengths of the fabrics coated with silica hybrid materials and of uncoated fabrics were obtained using the following relationships:

$$\text{Relative color strength (\%)} = \frac{K/S \text{ of treated sample}}{K/S \text{ of untreated sample}} \times 100\%$$

$$\Delta E = \sqrt{(\Delta L)^2 + (\Delta a)^2 + (\Delta b)^2}$$

where L is the lightness or shade of the dye, a is a measure of redness or greenness, and b is a measure of yellowness or blueness. It is noted that ΔL = L<sub>dyed</sub> – L<sub>undyed</sub>, Δa = a<sub>dyed</sub> – a<sub>undyed</sub>, and Δb = b<sub>dyed</sub> – b<sub>undyed</sub>.

The color difference between the largest and the smallest values of the same fabric was obtained, and these values indicate the color evenness of the fabrics. According to the regulation of the National Bureau of Standards (N.B.S.), the fabric is acceptable for use in industrial applications when the color difference is less than 2.0.

## RESULTS AND DISCUSSION

### FT-IR analysis of hybrid materials

In all the FT-IR spectra of hybrid materials A<sub>1</sub>–A<sub>4</sub>, as illustrated in Figure 1, a strong absorption band in the range 3413–3380 cm<sup>-1</sup> dominated, and the absorption peaks around 1628–1634 cm<sup>-1</sup> revealed that the hybrid materials had Ti–O groups that enabled the formation of a Ti–O–Ti network. These results are characteristic of the OH stretching vibrations of free and hydrogen-bonded surface hydroxyl groups. Water molecules can be strongly or weakly bound to the titania surface and form numerous broad OH stretching vibrations. In addition, in all the FT-IR spectra of hybrid materials T<sub>1</sub>–T<sub>4</sub>, as illustrated in Figure 2, a strong absorption band in the range 3435–3380 cm<sup>-1</sup> dominated, and the absorption peaks around 1628–1636 cm<sup>-1</sup> revealed that the hybrid materials had Ti–O groups that enabled the formation of a Ti–O–Ti network. A second typical absorption region for TiO<sub>2</sub> at 1200–1700 cm<sup>-1</sup> has been reported and was assigned to physically adsorbed water (H–O–H bending, peak at 1636 cm<sup>-1</sup>). The FT-IR spectra in Figure 1 show that hybrid material A<sub>1</sub> had an O–H group and a Ti–O group with absorption peaks near 3412 cm<sup>-1</sup> and 1636 cm<sup>-1</sup>, respectively. Additionally, the spectrum of Al–O showed strong absorption bands in the range 568–572 cm<sup>-1</sup>, verifying that the hybrid materials had Al–O groups. Thus, it is reasonable to assume that reactions occurred between boehmite and titania. The FT-IR spectra in Figure 1 show hybrid materials A<sub>1</sub>–A<sub>4</sub> with various boehmite/titania sol solution ratios. A high boehmite concentration increased the strength of the Al–O absorption and strengthened the bonding. The structure of Al–O–Al was analyzed using <sup>27</sup>Al-NMR.

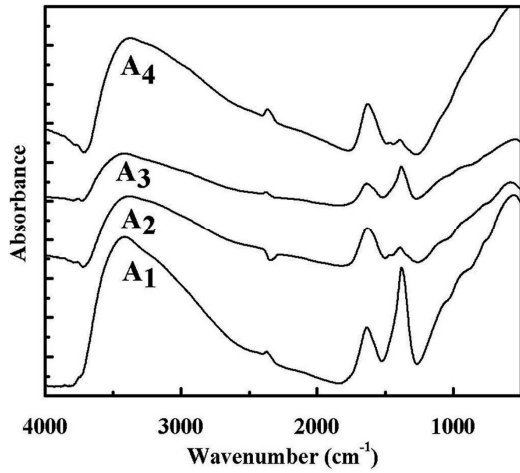


Figure 1: FT-IR spectra of hybrid materials A<sub>1</sub>–A<sub>4</sub>

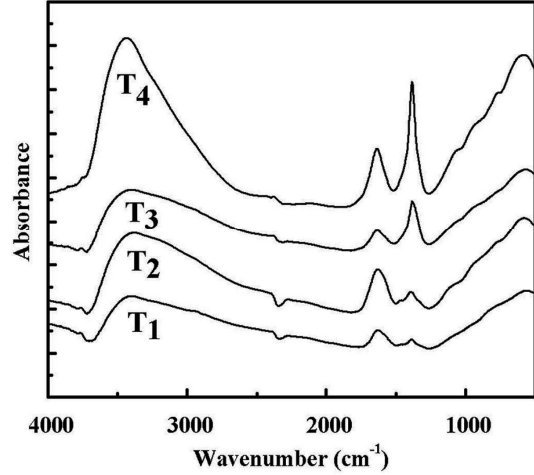


Figure 2: FT-IR spectra of hybrid materials T<sub>1</sub>–T<sub>4</sub>

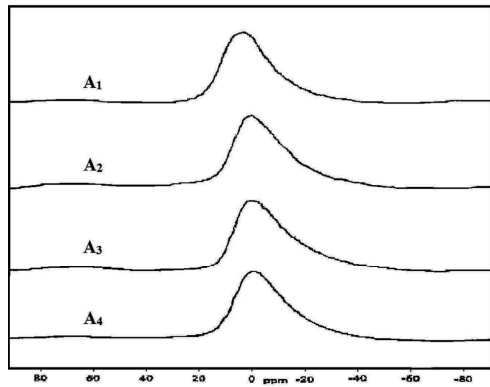


Figure 3: <sup>27</sup>Al-NMR spectra of hybrid materials A<sub>1</sub>–A<sub>4</sub>

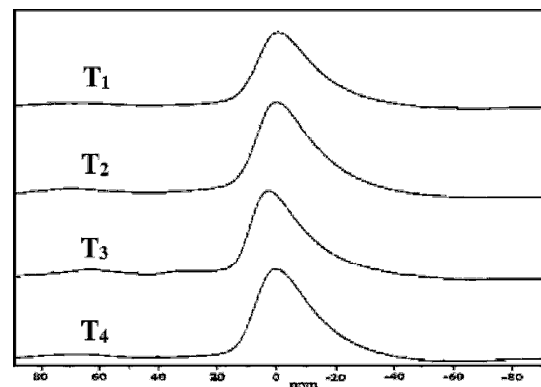


Figure 4: <sup>27</sup>Al-NMR spectra of hybrid materials T<sub>1</sub>–T<sub>4</sub>

### <sup>27</sup>Al-NMR analysis of hybrid materials

The <sup>27</sup>Al-NMR spectra of hybrid materials A<sub>1</sub>–A<sub>4</sub> (Figure 3) show that the structure formed during hydrolysis of the chemical precursor aluminum isopropoxide resulted in six-coordinated boehmite with absorption peaks corresponding to literature values in the range -10–10 ppm. Hybrid material A<sub>1</sub> had a single peak at -0.312 ppm, indicative of an octahedral coordination of Al atoms. There was also a very broad range of sidebands from which a quadrupolar coupling constant was derived, indicating a very high degree of disorder.<sup>34</sup> The six-coordinated boehmite in hybrid materials A<sub>2</sub>, A<sub>3</sub>, and A<sub>4</sub> absorbed at  $\delta = 1.086$  ppm,  $\delta = 0.535$  ppm, and  $\delta = 0.154$  ppm, respectively. NMR data were averaged for hybrid materials A<sub>1</sub>–A<sub>4</sub>, but

they were not characteristic of the surface where the heterogeneous reactions occurred. Furthermore, as shown in Figure 4, the six-coordinated boehmite in hybrid materials T<sub>1</sub>–T<sub>4</sub> absorbed at  $\delta = -0.257$  ppm,  $\delta = 1.086$  ppm,  $\delta = 0.283$  ppm, and  $\delta = 0.431$  ppm, respectively. The octahedral coordination of Al identified with MAS-NMR did not necessarily represent Al atoms near the surface, which could have been under-coordinated. As the AIP increased, the six-coordinated boehmite absorption peaks became irregular. Moreover, <sup>27</sup>Al-NMR was used to examine the structure that formed during the hydrolysis of Al. Although the FT-IR results indicated the formation of Al–O–Al during the sol-gel reaction, <sup>27</sup>Al solid-state NMR provided additional information about the structure of

boehmite in both hybrid materials A<sub>1</sub>–A<sub>4</sub> and T<sub>1</sub>–T<sub>4</sub> and the extent of the Al–OH condensation reaction.

#### EDS analysis of processed cotton fabrics

According to Table 1, the EDS (Energy dispersive X-ray spectroscopy) analysis of the processed cotton fabrics showed that the aluminium content decreased with increasing titania addition to processed cotton fabrics CA<sub>1</sub>–CA<sub>4</sub>. The elements oxygen and aluminum decreased at the maximum ratio of the hybrid material. This was because the high ratio formed more alumina film bonding Ti–O–Ti, and, as shown in Figure 5, the titanium content in hybrid material CA<sub>4</sub> increased suddenly. In addition, according to Table 1, the relatively large mole number of aluminium in the processed cotton fabrics CT<sub>1</sub>–CT<sub>4</sub> indicated a relatively high aluminium content, according to the EDS analysis. However, the increase in the mole number was small, and hence, each increment was small. According to Figure 6, the amount of aluminium increased in processed cotton fabrics CT<sub>4</sub>, but the difference was small. Therefore, a larger hybrid material ratio indicated that the alumina titania bonding Al–O–Ti was more obvious. According to Table 1, when the TBT was fixed, the titania

content decreased with an increase in the aluminium content. The maximum CT<sub>4</sub> level via  $\gamma$ -AlOOH addition in the processed cotton fabrics resulted in the maximum aluminium content.

#### Analysis of color strength and evenness of processed fabrics

Cotton fabrics were dyed with hybrid materials prepared using various ratios of  $\gamma$ -AlOOH to TBT. In Table 2, the  $\Delta E$  values of cotton fabrics processed with hybrid materials A<sub>1</sub>–A<sub>4</sub> and T<sub>1</sub>–T<sub>4</sub> range from 0.26 to 0.77. These values indicate that the evenness of the processed fabrics lies within the acceptable range.

The K/S value of unprocessed cotton fabrics was 9.85 and the K/S values of the fabrics processed with hybrid materials A<sub>1</sub>–A<sub>4</sub> and T<sub>1</sub>–T<sub>4</sub> ranged from 8.31 to 9.79. The values listed in Table 2 indicate that the amount of  $\gamma$ -AlOOH and TBT greatly affect the color strength of cotton fabrics; the higher the amount, the lower the color strength. Moreover, the addition of various ratios of  $\gamma$ -AlOOH to cotton fabrics during dyeing would result in a slightly better color strength than the addition of various ratios of TBT.

Table 1  
EDS analysis of hybrid materials CA<sub>1</sub>–CA<sub>4</sub>, CT<sub>1</sub>–CT<sub>4</sub>

Samples	Elemental composition (%)			
	C	O	Al	Ti
CA <sub>1</sub>	12.23	35.17	21.91	30.69
CA <sub>2</sub>	11.87	32.73	15.81	39.59
CA <sub>3</sub>	18.16	28.54	12.90	40.40
CA <sub>4</sub>	10.76	26.54	10.31	52.39
CT <sub>1</sub>	5.45	24.96	9.28	60.31
CT <sub>2</sub>	11.87	32.73	15.81	39.59
CT <sub>3</sub>	16.21	32.49	16.52	34.78
CT <sub>4</sub>	28.50	31.67	16.69	23.14

Table 2  
Color strength and evenness of processed cotton fabrics

Compd.	Color strength (K/S)	Evenness ( $\Delta E$ )	Compd.	Color strength (K/S)	Evenness ( $\Delta E$ )
CA <sub>1</sub>	9.54	0.66	CT <sub>1</sub>	9.79	0.73
CA <sub>2</sub>	8.79	0.53	CT <sub>2</sub>	8.79	0.53
CA <sub>3</sub>	8.46	0.42	CT <sub>3</sub>	8.49	0.26
CA <sub>4</sub>	8.31	0.77	CT <sub>4</sub>	8.36	0.48

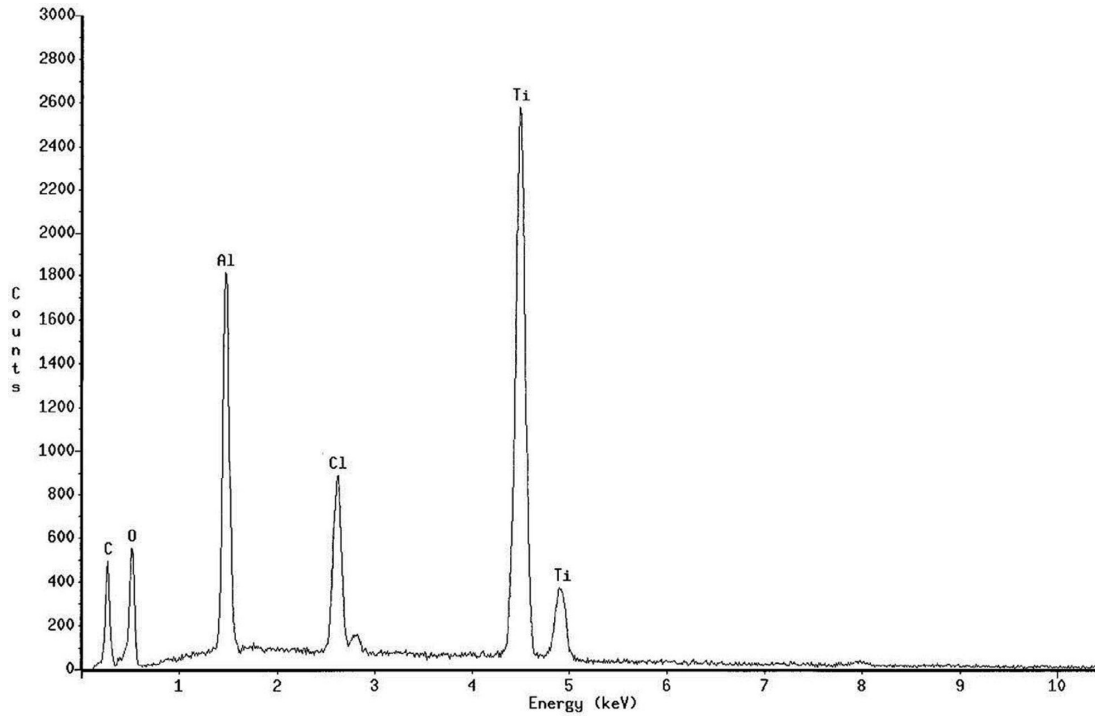


Figure 5: EDS diagram of processed fabrics CA<sub>4</sub>

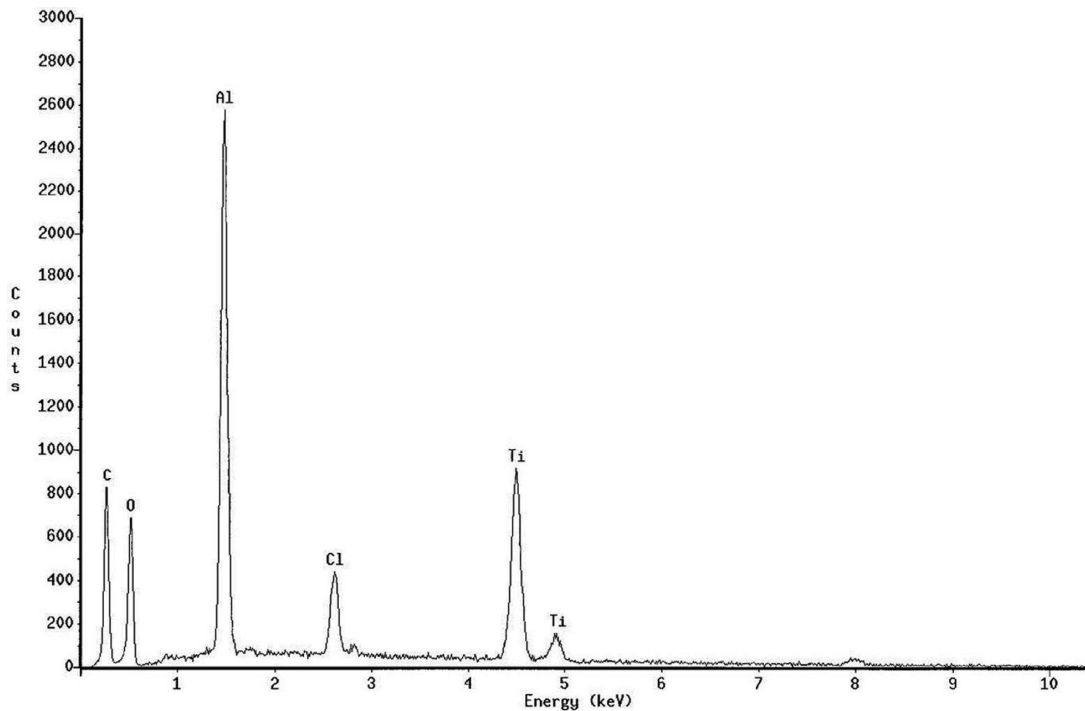


Figure 6: EDS diagram of processed fabrics CT<sub>4</sub>

### Surface morphology of processed cotton fabrics

We used a SEM to observe the surfaces of the cotton fabrics processed with hybrid materials A<sub>1</sub>–A<sub>4</sub> and T<sub>1</sub>–T<sub>4</sub>, and we then discussed the differences between the cotton fabrics dyed with

hybrid materials T<sub>1</sub>–T<sub>4</sub> with different amounts of aluminum gel and hybrid materials A<sub>1</sub>–A<sub>4</sub> with different amounts of tetrabutyl titanate.

First, we observed the grey cloth of cotton fabrics, which had not yet been dyed, as shown in

Figure 7(A). It was smooth and the space between yarns was rather large. Figures 7(B)–(E) show the surfaces of the cotton fabrics after being processed with hybrid materials,  $A_1$ – $A_4$ , respectively. According to these images, after being processed with hybrid material  $A_1$ , there were some chemical compounds attached to the fabric surface. The hybrid material created a uniform network-structured protection layer on the fabric surface. Larger amounts of aluminum gel led to more chemical compounds covering the fabric surface. In this way, the water repellency, electric conductivity, and mechanical properties of the fabrics could be improved. Figure 7(A) shows the SEM image of grey cloth  $A_0$ , which had not been

processed. According to the image, the surface was very smooth and the space between yarns was rather large. Figure 8(A) shows some small chemical compounds attached to the fabric surface after being processed with hybrid material  $T_1$ . The distribution of the compounds was not uniform and these compounds did not fill in the space perfectly. Therefore, the water repellency effect was not significant. Figures 8(B)–(D) are the SEM images of the fabrics processed with hybrid materials  $T_2$ – $T_4$ . According to the images, there were a lot of particles attached to the fabric surfaces. The fabric surfaces were covered. Therefore, the thicknesses of the fabrics increased. These large particles filled in the space and thus increased water repellency.

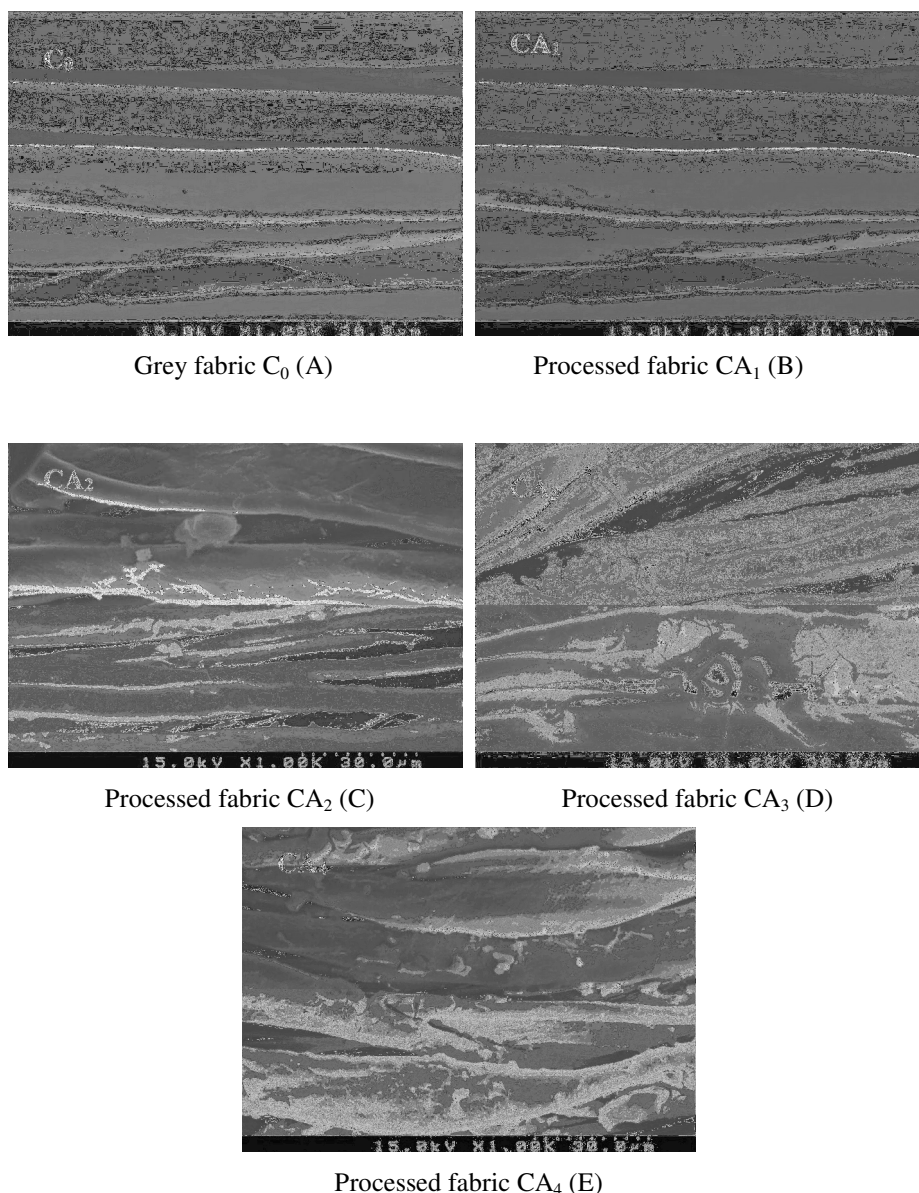


Figure 7: SEM image of grey cotton fabric and processed fabrics  $CA_1$ – $CA_4$  ( $\times 1000$ )

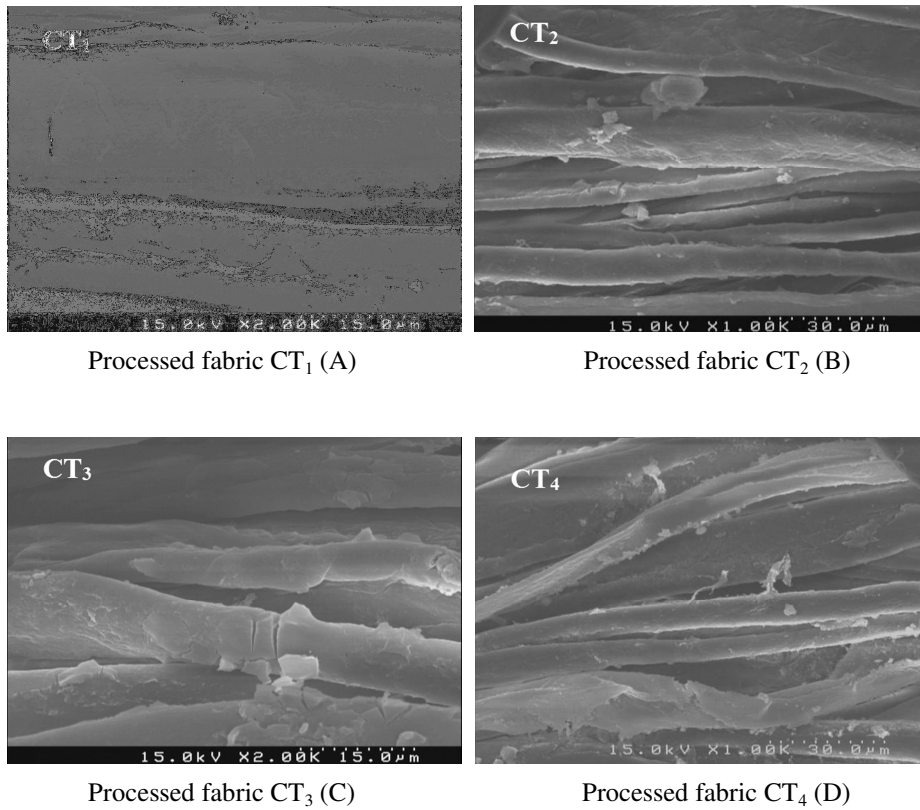


Figure 8: SEM image of processed fabrics CT<sub>1</sub>-CT<sub>4</sub> (×1000)

Table 3  
Conductivity analysis of grey fabrics and processed cotton fabrics CA<sub>1</sub>-CA<sub>4</sub>, CT<sub>1</sub>-CT<sub>4</sub>

Compd.	Conductivity (Ω)	Compd.	Conductivity (Ω)
cotton	$3.21 \times 10^9$	cotton	$3.21 \times 10^9$
CA <sub>1</sub>	$1.75 \times 10^8$	CT <sub>1</sub>	$2.63 \times 10^8$
CA <sub>2</sub>	$3.35 \times 10^7$	CT <sub>2</sub>	$3.35 \times 10^7$
CA <sub>3</sub>	$4.08 \times 10^7$	CT <sub>3</sub>	$2.58 \times 10^7$
CA <sub>4</sub>	$4.74 \times 10^8$	CT <sub>4</sub>	$4.05 \times 10^6$

**Conductivity analysis for dyed fabrics**

Dyed fabrics with composite materials of different ratios were applied to cotton fabrics. According to the results of the experiments summarized in Table 3, the resistance of the original cloth was very high, i.e.  $3.21 \times 10^9 \Omega$ ; this high value implies that the original fabrics are not electrically conductive. Table 3 also shows that, on the basis of electric conductivity analysis of composite materials with a fixed amount of aluminum isopropoxide and varying amounts of tetrabutyl titanate, the resistance was not significantly different from that of the original fabrics. It was inferred that increasing the amount of titanium gel was not very helpful in decreasing

the resistance. The electric conductivity of the cotton fabrics was not significantly improved.

According to Table 3, on the basis of electric conductivity analysis of composite materials with a fixed amount of tetrabutyl titanate and different amounts of aluminum isopropoxide, the resistance decreased as the amount increased. The resistance of CT<sub>4</sub> was  $4.05 \times 10^6 \Omega$ , which was rather low. This result shows that the resistance could be decreased by increasing the amount of aluminum gel. The best result was observed for a 1000-fold decrease in resistance. Thus, it could be inferred that by mixing aluminum gels, the conductivity of cotton fabrics increases. After comparing the two series of composite materials, it was found that the



resistance performance was better with tetrabutyl titanate. The data show that aluminum isopropoxide

could indeed improve the electric conductivity of cotton fabrics.

Table 4  
Surface hydrophobicity evaluation of hybrid materials processed on PET fabrics CA<sub>1</sub>–CA<sub>4</sub>, CT<sub>1</sub>–CT<sub>4</sub>

Compd.	Contact angle (degree)		Compd.	Contact angle (degree)	
	Before washing	After washing		Before washing	After washing
cotton	0	0	--	--	--
CA <sub>1</sub>	117.5	114	CT <sub>1</sub>	109.5	105
CA <sub>2</sub>	114	110	CT <sub>2</sub>	114	110
CA <sub>3</sub>	112	109	CT <sub>3</sub>	120.5	111
CA <sub>4</sub>	109	103	CT <sub>4</sub>	126.5	118

Table 5  
Weathering assessment of cotton processed fabrics

Compd.	UV irradiated	UV irradiated	Compd.	UV irradiated	UV irradiated
	for 8 h	for 16 h		for 8 h	for 16 h
cotton	2-3	1	--	--	--
CA <sub>1</sub>	3-4	3-4	CT <sub>1</sub>	3-4	3-4
CA <sub>2</sub>	3-4	3-4	CT <sub>2</sub>	4	3-4
CA <sub>3</sub>	4	4	CT <sub>3</sub>	4	3-4
CA <sub>4</sub>	4-5	4	CT <sub>4</sub>	4-5	4

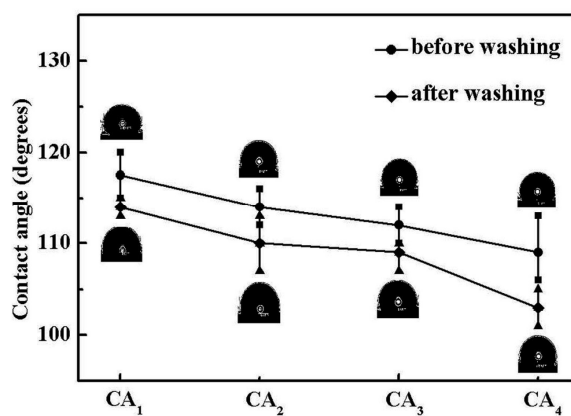


Figure 9: Contact angle analysis of cotton fabrics CA<sub>1</sub>–CA<sub>4</sub>

### Contact angle analysis of dyed fabrics

As shown in Figure 9, the grey cloth used for cotton fabrics was not water repellent, and its contact angle was 0°. The processed fabrics CA<sub>1</sub>–CA<sub>4</sub> were made of hybrid materials composed of a fixed amount of boehmite sol and different amounts of tetrabutyl titanate. Their contact angles were between 109° and 117.5°. It can be inferred that tetrabutyl titanate may increase the contact angle from 109° to 117.5°. Processed fabrics

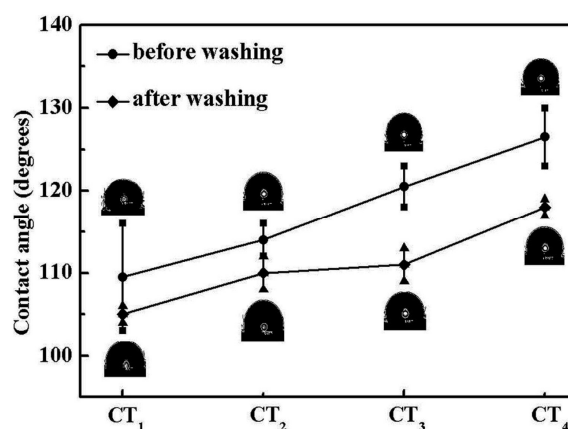


Figure 10: Contact angle analysis of cotton fabrics CT<sub>1</sub>–CT<sub>4</sub>

CT<sub>1</sub>–CT<sub>4</sub> were made of hybrid materials composed of a fixed amount of tetrabutyl titanate and different amounts of boehmite sol. As shown in Figure 10, their contact angles were between 109.5° and 126.5°. It can be inferred that it was more effective to change the amount of boehmite sol, while keeping the amount of tetrabutyl titanate fixed. The contact angle increased with the amount of AIP added, increasing from 109.5° to 126.5°. Generally speaking, the contact angle of processed fabric CT<sub>4</sub>

with the higher amount of boehmite sol was  $126.5^\circ$ , which was higher than  $117.5^\circ$ , the contact angle of processed fabric CA<sub>4</sub>. This could be because the water repellency of the Al–O–Al 6-coordinate network structure was better than that of the Ti–O–Ti four-coordinate network structure. In addition, because the Al–O–Ti hybrid material created a strong protection layer on the surface of the cotton fabrics to improve the physical properties of the cotton fabrics, it was concluded that boehmite sol and tetrabutyl titanate possessed water repellent functions. Moreover, as shown in Table 4, after 10 washing tests, the angle difference for processed fabrics CA<sub>1</sub>–CA<sub>4</sub> before and after washing was  $6^\circ$ . For processed fabrics CT<sub>1</sub>–CT<sub>4</sub>, it was  $8^\circ$ . Although the contact angle slightly decreased, the protection film created with boehmite sol and tetrabutyl titanate kept the water repellency level at 3~4. Both boehmite sol and tetrabutyl titanate could help in increasing the effectiveness of water repellency.

#### Weathering of cotton fabrics with hybrid materials

This study followed the ASTM G154 standard practice to conduct experiments for resistance to elements. The hybrid materials of different ratios of composites were applied to the cotton fabrics. According to the results of the experiments summarized in Table 5, the UV resistance of the cotton fabrics processed with the hybrid materials was better than that of the non-processed cotton fabrics. After 64 h of UV exposure, it was found that the UV resistance levels of the fabrics processed with the hybrid materials of different composite ratios were of about 3. The UV resistance levels of the fabrics processed with A<sub>1</sub> and A<sub>2</sub> were of 4-5, which was quite high. Thus, the UV resistance of the fabrics processed with the hybrid material could be improved by fixing the amount of tetrabutyl titanate and changing the amount of aluminum isopropoxide. After comparing this hybrid material with tetrabutyl titanate, it was found that this hybrid material helped in increasing the UV resistance more.

#### CONCLUSION

Boehmite/titania hybrid materials were synthesized using a hydrothermal process with various molar ratios of aluminum isopropoxide and titanium-n-butoxide chemical precursors. Next, the

sol solutions were applied to the cotton fabrics to explore the properties of the processed cotton fabrics. According to the results of the experiments, after the reaction with the aluminum isopropoxide/tetrabutyl titanate hybrid materials, a thick and sticky transparent fluid layer covered the surface. After the FTIR and <sup>27</sup>Al-NMR analyses, it was confirmed that this fluid was formed with the Al–O–Al and Al–O–Ti bonds of the hybrid materials. The results of the electric conductivity analyses with fixed amounts of tetrabutyl titanate and different amounts of aluminum isopropoxide show that the electric conductivities of the processed cotton fabrics can be increased by a 1000-fold decrease in resistance. However, the results of the electric conductivity analyses with a fixed amount of aluminum isopropoxide and different amounts of tetrabutyl titanate show no significant change in electric conductivity. The levels of resistance of the elements of the fabrics processed with a fixed amount of aluminum isopropoxide and different amounts of tetrabutyl titanate were of about 4~5, whereas those of the fabrics processed with a fixed amount of tetrabutyl titanate and different amounts of aluminum isopropoxide were of about 4. According to the results of the contact angle tests, the contact angles of the fabrics processed with a fixed amount of aluminum isopropoxide and different amounts of tetrabutyl titanate were of about  $109^\circ$ – $117.5^\circ$ , and after 10 washes the contact angles were of  $103^\circ$ – $114^\circ$ . On the other hand, the contact angles of the fabrics processed with a fixed amount of tetrabutyl titanate and different amounts of aluminum isopropoxide were of about  $109.5^\circ$ – $126.5^\circ$ , and after 10 washes the contact angles were of  $105^\circ$ – $108^\circ$ . Further, the water repellency levels of the processed cotton fabrics with a protection layer produced by boehmite sol and titanium dioxide were about of 3~4.

**ACKNOWLEDGMENTS:** The authors would like to thank the National Science Council of the Republic of China, Taiwan, for financially supporting this research under Contract No. NSC-100-2622-E-168-001-CC3.

#### REFERENCES

- <sup>1</sup> C. Sanchez, B. Julian, P. Belleville and M. Popall, *J. Mater. Chem.*, **15**, 3559 (2005).
- <sup>2</sup> K. H. Haas, *Adv. Eng. Mater.*, **2**, 571 (2000).
- <sup>3</sup> J. Zhu, B. Y. Tay and J. Ma, *J. Mater. Process. Tech.*, **192-193**, 561 (2007).

- <sup>4</sup> K. Byrappa, A. K. Subramani, S. Ananda, K. M. L. Rai, M. H. Sunitha *et al.*, *J. Mater. Sci.*, **41**, 1355 (2006).
- <sup>5</sup> S. Y. Wu, W. Zhang and X. M. Chen, *J. Mater. Sci. Mater. El.*, **21**, 450 (2010).
- <sup>6</sup> J. Choi, S. Komarneni, K. Grover, H. Katsuki and M. Park, *Appl. Clay Sci.*, **46**, 69 (2009).
- <sup>7</sup> R. Pazik, D. Hreniak and W. Strek, *Mater. Res. Bull.*, **42**, 1188 (2007).
- <sup>8</sup> J. Q. Xu, Y. P. Chen, Y. D. Li and J. N. Shen, *J. Mater. Sci.*, **40**, 2919 (2005).
- <sup>9</sup> Y. H. Han, A. Taylor, M. D. Mantle and K. M. Knowles, *J. Non-Cryst. Solids*, **353**, 313 (2007).
- <sup>10</sup> G. Jin, Y. Tang, S. Liu, S. Wang and R. Xing, *Anal. Lett.*, **41**, 1811 (2008).
- <sup>11</sup> M. S. Yen, *Int. J. Polym. Mater.*, **60**, 893 (2011).
- <sup>12</sup> R. Doufnoune and N. Haddaoui, *Int. J. Polym. Mater.*, **55**, 815 (2006).
- <sup>13</sup> K. H. Haas, *Adv. Eng. Mater.*, **2(9)**, 571 (2000).
- <sup>14</sup> T. Jesionowski, *Dyes Pigments*, **55**, 133 (2002).
- <sup>15</sup> D. Donescu, M. Teodorescu, S. Serban, L. Fusulan and C. Petcu, *Eur. Polym. J.*, **35**, 1679 (1999).
- <sup>16</sup> R. J. Watts, S. Kong, M. P. Orr, G. C. Miller, and B. E. Henry, *Water Res.*, **29**, 95 (1995).
- <sup>17</sup> M. R. Hoffmann, S. T. Martin, W. Choi and D. W. Bahnemann, *Chem. Rev.*, **95**, 69 (1995).
- <sup>18</sup> A. Fujishima, T. N. Rao and D. A. Tryk, *J. Photoch. Photobio. C*, **1**, 1 (2000).
- <sup>19</sup> B. Ohtani, Y. Ogawa and S. Nishimoto, *J. Phys. Chem. B*, **101**, 3746 (1997).
- <sup>20</sup> S. Sakthivel, B. Neppolian, M. V. Shankar, B. Arabindoo, M. Palanichamy *et al.*, *Sol. Energ. Mat. Sol. C*, **77**, 65 (2003).
- <sup>21</sup> A. Fujishima and K. Honda, *Nature*, **238**, 37 (1972).
- <sup>22</sup> P. C. Maness, S. Smolinski, D. M. Blake, Z. Huang, E. J. Wolfrum *et al.*, *Appl. Environ. Microb.*, **65(9)**, 4094 (1999).
- <sup>23</sup> P. V. Kamat and D. Meisel, *Curr. Opin. Colloid In.*, **7**, 282 (2002).
- <sup>24</sup> J. Patrick and S. Clement, *J. Mater. Chem.*, **6(4)**, 511 (1996).
- <sup>25</sup> C. L. Jackson, B. J. Bauer, A. I. Nakatani and J. D. Barnes, *Chem. Mater.*, **8**, 727 (1996).
- <sup>26</sup> C. Xia, F. Wu, Z. Meng, F. Li, D. Peng *et al.*, *J. Membrane Sci.*, **116**, 9 (1996).
- <sup>27</sup> W. Zhang, W. Liu and C. Wang, *Ceram. Int.*, **29**, 427 (2003).
- <sup>28</sup> T. Mousavand, S. Ohara, M. Umetsu, J. Zhang, S. Takami *et al.*, *J. Supercrit. Fluid.*, **40**, 397 (2007).
- <sup>29</sup> A. Torncrona, J. Brandt, L. Lowendahl and J. E. Otterstedt, *J. Eur. Ceram. Soc.*, **17**, 1459 (1997).
- <sup>30</sup> Z. He, J. Mab and G. E. B. Tan, *J. Alloy. Compd.*, **486**, 815 (2009).
- <sup>31</sup> T. Kiyoharu, K. Noriko and M. Tsutomu, *J. Amer. Ceram. Soc.*, **80(12)**, 3213 (1997).
- <sup>33</sup> B. E. Yoldas, *Ceram. Bull.*, **54**, 289 (1975).
- <sup>33</sup> V. R. G. Dev, J. Venugopal, S. Sudha, G. Deepika and S. Ramakrishna, *Carbohydr. Polym.*, **75**, 646 (2009).
- <sup>34</sup> E. Kemnitz, U. Groß, S. Rudiger and C. S. Shekar, *Angew. Chem. Int. Edit.*, **42**, 4251 (2003).